CARBON 47 (2009) 912–916

available at www.sciencedirect.com

ScienceDirect

journal homepage: www.elsevier.com/locate/carbon

Letter to the Editor

Flame synthesis of carbon nanotubes using a double-faced wall stagnation flow burner

*Sang Kil Woo, Young Taek Hong, Oh Chae Kwon**

School of Mechanical Engineering, Sungkyunkwan University, 300 Chunchun-dong, Jangan-gu, Suwon, Kyunggi-do 440-746, Korea

ARTICLE INFO

Article history:
Received 1 May 2008
Accepted 28 November 2008
Available online 13 December 2008

ABSTRACT

The potential of using a double-faced wall stagnation flow (DWSF) burner in mass production of multi-walled carbon nanotubes (MWCNTs) has been evaluated. Due to minimized heat losses across a catalyst plate and redistributed temperature profiles on the plate surface, the DWSF burner can produce abundant and uniform MWCNTs, the quality and yield of synthesized MWCNTs being controlled by varying flame stretch rates.

Because of the unique mechanical and electrical properties of carbon nanotubes (CNTs), there has been substantial interest in their synthesis and use for a wide variety of new applications [1]. Recently there has been increasing interest in mass production of CNTs by catalytic combustion [2–6], focusing on the fundamental aspects of combustion synthesis of CNTs for various flame configurations. Considering that the combustion synthesis methods have potential for mass production of CNTs, however, a unique method that can be directly applicable to mass production of CNTs should be developed. We propose herein a flame configuration towards enabling mass production of CNTs. A double-faced wall stagnation flow (DWSF) burner establishes a premixed flame above each side of a stagnation wall since the diluted fuel-air premixtures injected through upper and lower nozzles are ignited, respectively (see Fig. 1). The combustion synthesis of CNTs on the DWSF burner appears to possess some potentially beneficial characteristics for mass production of CNTs: minimized heat losses due to two flames generated along both surfaces of the stagnation plate wall and redistributed temperature profiles on the wall surfaces by properly controlling stretch rates of flames through changing mass flow rates of premixtures at the upper and lower nozzles or the distance between the nozzle and the wall. Thus, in the present investigation we aim to study the potential of improving mass production of CNTs by using a DWSF burner.

A diagram of the present experimental apparatus appears in Fig. 1, which consists of upper and lower tubes (SS304 tubes with inner diameter of 3 mm and the passage length/diameter ratio of 100 to help insure fully-developed pipe flow at the tube exit) surrounded by water-cooling pipes, a stagnation wall (a nickel (Ni)-coated (electroless plated) stainless steel disk with diameter of 45 mm and thickness of 1 mm), a reactant mixture supply system, thermocouples (R-type) for measuring temperature distribution on the stagnation wall surface, and a digital camera (Nikon D70) for recording the flame images. Nitrogen (N_2)-diluted ethylene (C_2H_4)/air premixture jets issued from tubes are impinged on a flat stagnation wall and then spark-ignited at temperature $T = 298 \pm 3$ K and atmospheric pressure (NTP) so that premixed flames are formed above both the wall surfaces. The Ni-coated plate surface heated by the flames is exposed to the premixture: the exposure time varies from 1 to 5 min since time to accumulate a certain quantity of the CNTs on the surface is up to the test condition. Commercial mass flow controllers (Area: 2 and 4 slm) with accuracy ±1% of full scale deliver the combustible mixture to the tubes: they are commanded by a PC-based software (LabView) that enables independent

* *Corresponding author:* Fax: +82 31 290 5889.
E-mail address: okwon@skku.edu (O.C. Kwon).
0008-6223/$ - see front matter
doi:10.1016/j.carbon.2008.11.052

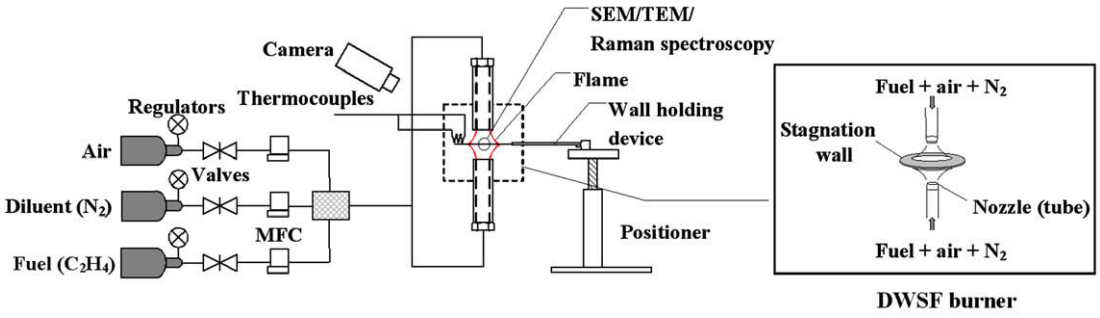

Fig. 1 – Schematic of experimental apparatus for the CNT synthesis.

control of mixture composition (i.e., fuel-equivalence ratio ϕ) and tube exit velocity V. Varying the jet velocities at the tube exit, flame stretch rates can be controlled within a range of stabilizing stationary flames. The global stretch rate is defined as follows: $\kappa = V/s$, where s is the distance between the stagnation plate and the tube exit. Experiments were carried out for $\phi = 1.7$ and $V = 1.8$–9.9 m/s at a fixed value of $s = 6.0$ mm, resulting in $\kappa = 298$–$1648\ s^{-1}$: s was determined from various pretests for properly generating CNTs. Synthesized CNTs were analyzed using FE-SEM (Philips ESEM-FEG-XL30), FE-TEM (Joel JEM2100F) and Raman spectroscopy (RS, Kaiser Optical RS).

Fig. 2 shows the FE-SEM and FE-TEM images and Raman spectra of the CNTs formed on the Ni-coated plate surface at the radius from the center of top surface of plate $r_u = 17$ mm and the radius from the center of bottom surface of plate $r_l = 8$ mm for a premixed $C_2H_4/O_2/N_2$ flame of $\phi = 1.7$ and the volumetric O_2 concentration in the nonfuel gases

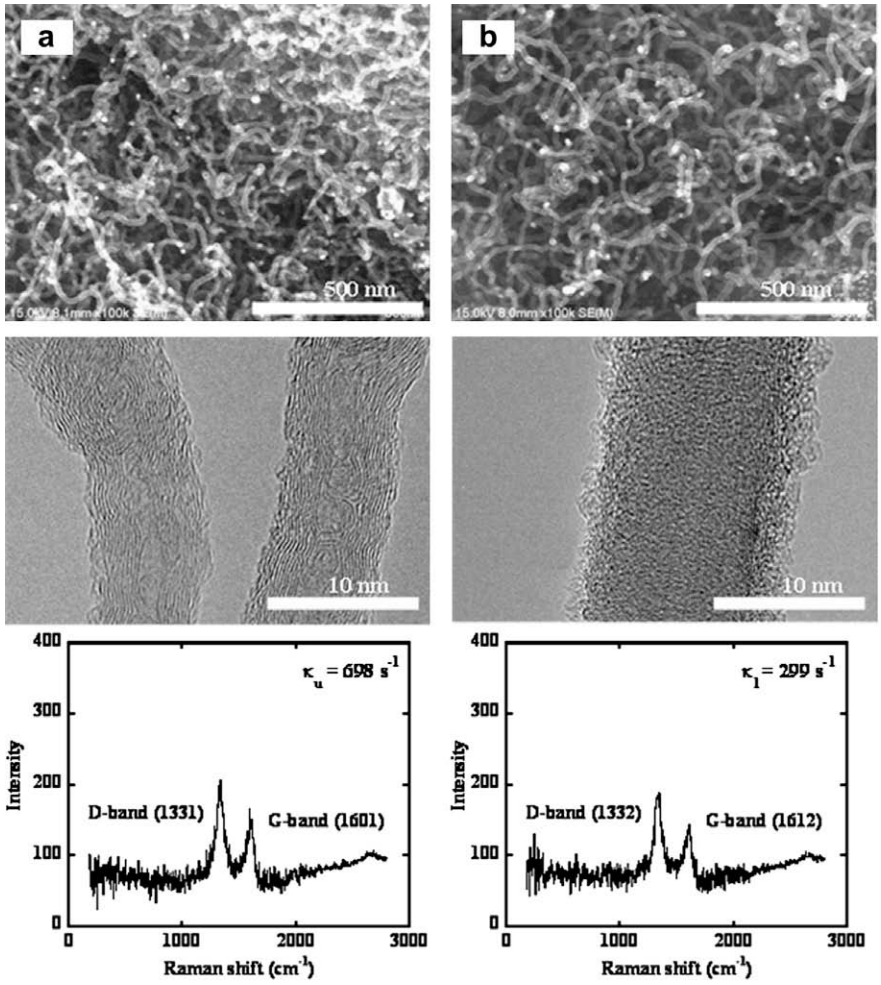

Fig. 2 – FE-SEM and FE-TEM images and Raman spectra of the CNTs formed at $r_u = 17$ mm on the top surface (a) and at $r_l = 8$ mm on the bottom surface (b) of a DWSF burner ($C_2H_4/O_2/N_2$ flame): $\phi = 1.7$, $X_{O2} = 0.107$, $V_u = 4.2$ m/s, $V_l = 1.8$ m/s and $s = 6.0$ mm ($\kappa_u = 698\ s^{-1}$ and $\kappa_l = 299\ s^{-1}$).

$X_{O2} = 0.107$ in a DWSF burner: the upper tube exit velocity $V_u = 4.2$ m/s and the lower tube exit velocity $V_l = 1.8$ m/s, resulting in the stretch rate of upper flame $\kappa_u = 698\ s^{-1}$ and the stretch rate of lower flame $\kappa_l = 299\ s^{-1}$ respectively. The different stretch rates for the upper and lower flames were determined by balancing the CNT-generated regions (unbalanced for the same stretch rate, due to buoyancy effects) on the top and bottom surfaces: for various conditions, the ratio of upper to lower stretch rates of 2.3 was effective for balancing the regions. The images indicate that the synthesized carbon materials are multi-walled CNTs (MWCNTs) with the diameters in the range of several to tens nanometers. Observing various TEM images, the present MWCNTs seem to grow according to a hollow-cored tip growth model due to a weak affinity of Ni for carbon [5]. The MWCNTs are observed in doughnut-shaped regions of $r = 10$–20 and 8–11 mm, respectively for the top and bottom surfaces which are broadened, compared with those for the corresponding single-faced wall stagnation flow (SWSF) burners shown in Fig. 3 ($r = 8$–9 and 12–17 mm respectively for the upwardly and downwardly issued SWSF burners). The FE-SEM images show that the qual-

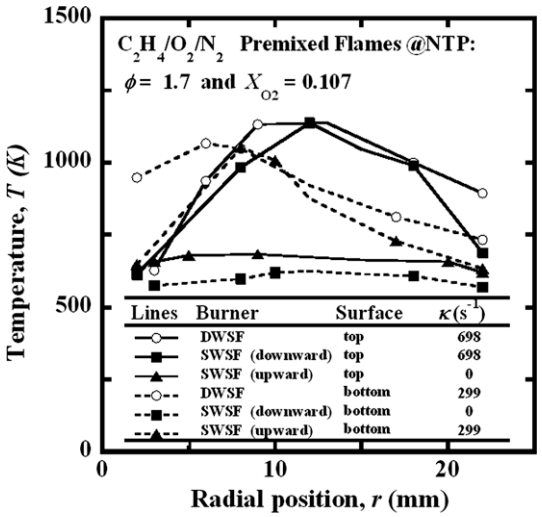

Fig. 4 – Measured temperature distributions along the stagnation plate surface for the flames used in Figs. 2 (a DWSF burner) and 3 (SWSF burners).

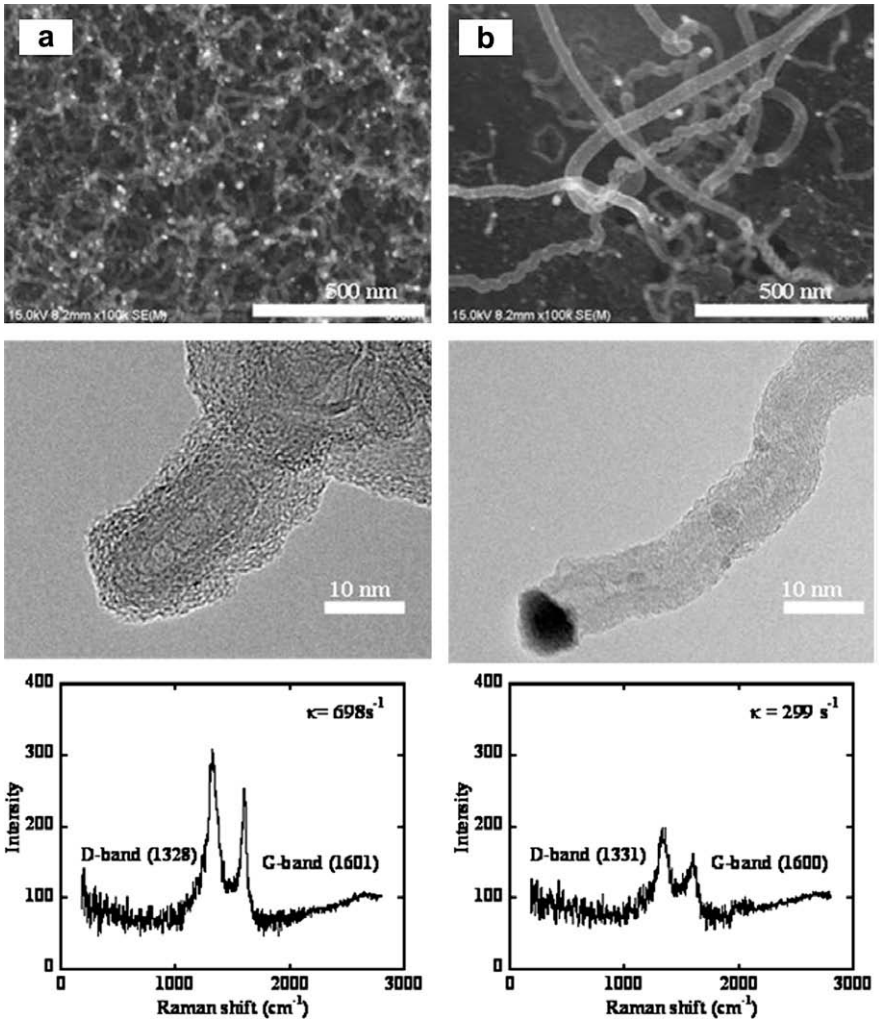

Fig. 3 – FE FE-SEM and FE-TEM images and Raman spectra of the CNTs formed on the plate surface of SWSF burners ($C_2H_4/O_2/N_2$ flames): (a) $r = 17$ mm, $\phi = 1.7$, $V = 4.2$ m/s, $s = 6.0$ mm ($\kappa = 698\ s^{-1}$) and $X_{O2} = 0.107$ (a downwardly issued SWSF burner) and (b) $r = 9$ mm, $\phi = 1.7$, $V = 1.8$ m/s, $s = 6.0$ mm ($\kappa = 299\ s^{-1}$) and $X_{O2} = 0.107$ (an upwardly issued SWSF burner).

ity of the DWSF burner-generating CNTs is relatively uniform, compared with that for the SWSF burners. The upwardly issued SWSF burner produces the most nonuniform, large-diameter and low-density (yield) CNTs, compared with the other burners. Fig. 4 shows temperature distributions on the stagnation wall surface for the conditions of Figs. 2 and 3. For the upwardly issued SWSF burner, temperature on the wall surface is lowest (i.e., the narrowest CNT synthesis region) and most nonuniform within the region for appropriate CNT synthesis temperature condition (>950 K), and the temperature difference across the plate is smallest, implying more heat losses to the ambient air across the plate due to buoyancy effects. The exposure time to obtain the CNTs from the DWSF burner is 3 min, which is shortened than that for the corresponding SWSF burners (5 min). Thus, the unique configuration of the DWSF burner-generating flames improves the quality and yield of CNTs compared with the corresponding SWSF burner-generating ones through minimizing heat losses across the catalyst plate and redistributing temperature profiles on the wall surfaces. The present results show no temperature dependence of the CNT diameter since the diameter significantly varies even for similar CNT-synthesized plate surface temperature in both SWSF and DWSF burners, implying that temperature cannot be considered a critical parameter influencing the quality of synthesized CNTs once it is within the range for appropriate CNT synthesis temperature condition. Instead, the heat losses to the ambient air across the plate and the temperature gradient along the plate (rather than temperature) within the temperature range for appropriate CNT synthesis seem to affect the quality of synthesized CNTs.

Experiments to observe if the quality and yield of synthesized CNTs can be controlled by varying the flame stretch rate were conducted for the same mixture and DWSF burner as in

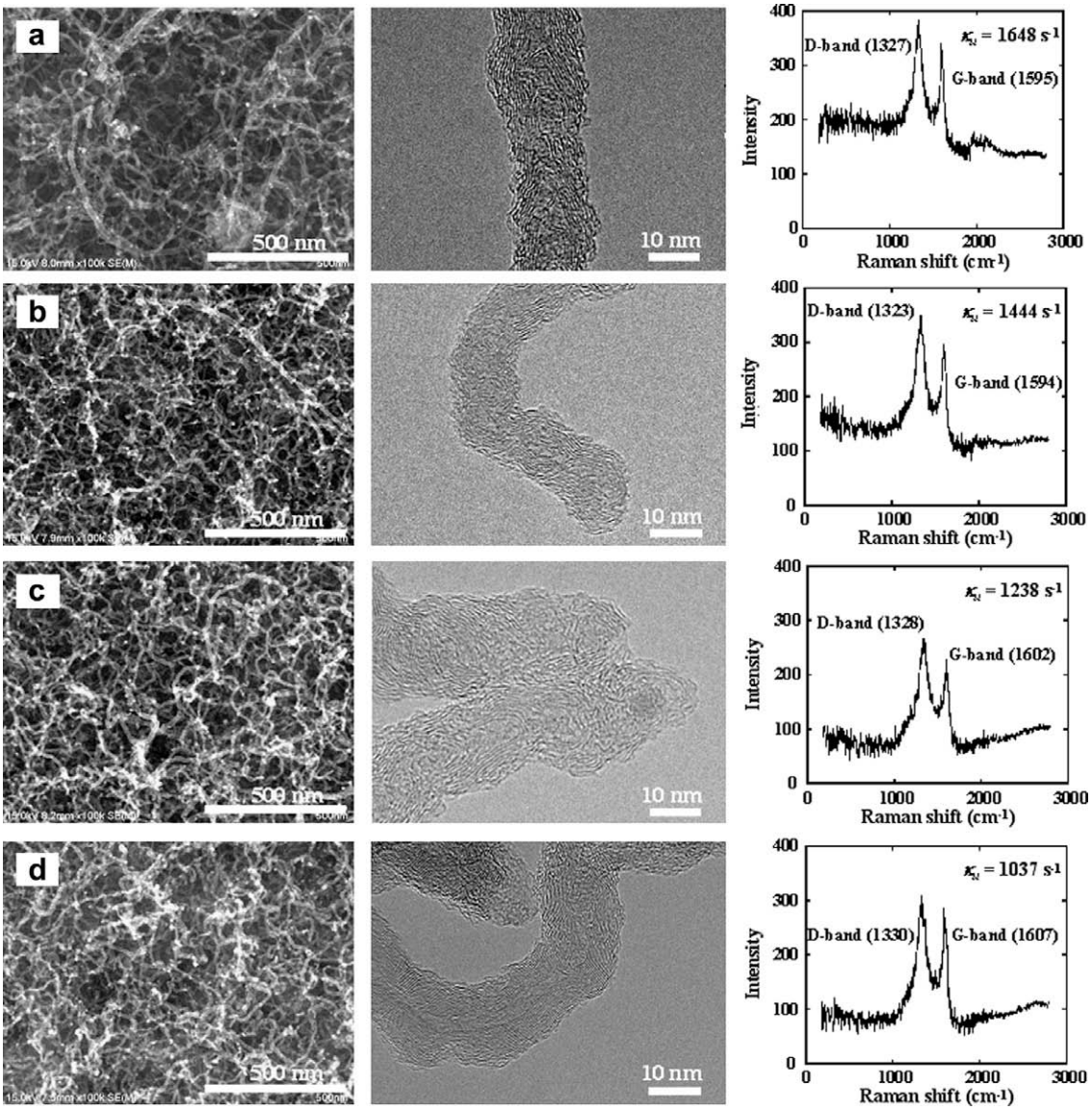

Fig. 5 – Effects of flame stretch rates on the formation of CNTs (for the same mixture and DWSF burner as in Fig. 2): (a) $\kappa_u = 1648\ s^{-1}$ and $\kappa_l = 706\ s^{-1}$, (b) $\kappa_u = 1444\ s^{-1}$ and $\kappa_l = 619\ s^{-1}$, (c) $\kappa_u = 1238\ s^{-1}$ and $\kappa_l = 530\ s^{-1}$, and (d) $\kappa_u = 1037\ s^{-1}$ and $\kappa_l = 444\ s^{-1}$. FE-SEM and FE-TEM images and Raman spectra of the CNTs formed at $r = 17$ mm on the top surface are shown.

Fig. 2 but for various stretch rates. The CNTs synthesized at $r_u = 17$ mm on the top surface of plate are shown in Fig. 5. The exposure time to obtain the CNTs was 1–3 min, decreasing with increasing stretch rates. The CNT-synthesized, doughnut-shaped region is broadened with increasing stretch rates, e.g., $r = 9$–21 and 10–13 mm respectively on the top and bottom surfaces for a high stretch rate condition ($\kappa_u = 1444\ s^{-1}$ and $\kappa_l = 619\ s^{-1}$). Since the amount of fuel provided onto the catalyst plate increases with increasing stretch rates, this tendency seems to be reasonable. According to FE-SEM images, the synthesized CNT density is nearly constant with stretch rates. Thus, higher stretch rates are better for more yields of CNTs unless the outer boundary of the CNT-synthesized region reaches the circumference of the plate. The averaged CNT diameter (that was obtained by direct measurement of the FE-SEM images at several locations within the CNT-generated region) is almost constant for stretch rates. However, the deviations increase with increasing stretch rates, indicating the degraded uniformity of CNTs. FE-TEM images show that the morphological feature of CNTs changes from straight to bamboo-shaped with increasing stretch rates. Thus, depending on the preferred quality of CNTs, we can determine the stretch rate of flame. The ratio of the intensities of D-band to G-band in the Raman spectra, which represents the degree of graphitization (crystallization) of synthesized CNTs [7], dose not show any tendency with stretch rates. Nearly constant heat losses to the ambient air across the plate for various stretch rates are observed from temperature distributions along the stagnation plate top and bottom surfaces for the conditions in Fig. 5 (not shown here). In conclusion, the proposed DWSF burner-generating flame enables mass production of CNTs, the quality and yield of synthesized CNTs being controlled by varying the flame stretch rate, e.g., large and nonuniform CNTs for enhanced heat losses across the plate, and nonuniform but more CNTs without any significant diameter change for enhanced stretch rates without heat loss change.

Acknowledgement

This work was supported by the Korean Research Foundation Grant (KRF-2006-311-D00341) funded by the Korean Government (MOEHRD).

REFERENCES

[1] Kruis FE, Fissan H, Peled A. Synthesis of nanoparticles in the gas phase for electronic, optical and magnetic applications – a review. J Aerosol Sci 1998;29(25):511–35.
[2] Vander Wal RL, Lee JH, Berger GM. The chemistry of premixed flame synthesis of carbon nanotubes using supported catalysts. Proc Combust Inst 2002;29:1079–85.
[3] Merchan-Merchan W, Saveliev A, Kennedy LA. Flame nanotube synthesis in moderate electric fields: from alignment and growth rate effects to structural variations and branching phenomena. Carbon 2006;44(15):3308–14.
[4] Lee GW, Jurng J, Hwang J. Formation of Ni-catalyzed multi-walled carbon nanotubes and nanofibers on a substrate using an ethylene inverse diffusion flame. Combust Flame 2004;139(1–2):167–75.
[5] Pan C, Liu Y, Cao F, Wang J, Ren Y. Synthesis and growth mechanism of carbon nanotubes and nanofibers from ethanol flames. Micron 2004;35(6):461–8.
[6] Nakazawa S, Yokomori T, Mizomoto M. Flame synthesis of carbon nanotubes in a wall stagnation flow. Chem Phys Lett 2005;403:158–62.
[7] Qi X, Ruan X, Pan C. Graphitization of solid carbon nanofibers at an unexpectedly low temperature. Mater Lett 2007;61:4272–5.